

MEASUREMENTS OF X_{\max} AND TESTS OF HADRONIC INTERACTIONS WITH THE PIERRE AUGER OBSERVATORY

C. Bleve* for the Pierre Auger Collaboration[†]

**Bergische Universität Wuppertal, FB C Physik, Gaußstr. 20, D-42097 Wuppertal, Germany*

[†]*Observatorio Pierre Auger, Av. San Martín Norte 304, 5613 Malargüe, Argentina*

full author list at http://www.auger.org/archive/authors_2011_3.html

The Pierre Auger Observatory is designed to detect the particle showers produced in the atmosphere by the most energetic cosmic rays, particles with individual energies up to $E \simeq 10^{20}$ eV. The challenge is to measure their spectrum, arrival directions and mass composition. The depth of the maximum of the longitudinal shower development (X_{\max}) is an indicator of the elemental composition. We present the measurement of the first two moments of the X_{\max} distribution for $E > 10^{18}$ eV. The interpretation in terms of primary masses can only be done by comparison with predictions of hadronic interaction models. The description of hadronic interactions can be tested by determining the muon content of air shower data. Our results at $E \sim 10^{19}$ eV are compared with the predictions of the QGSjetII model for both proton and iron primaries, showing an observed excess of muons with respect to the model.

1 Introduction

Cosmic rays (CR) are a natural beam of ionized atomic nuclei with a rapidly falling energy spectrum that extends up to $E \sim 10^{20}$ eV. To understand the sources and propagation of CRs, the measurement of their flux, elemental composition and distribution of arrival directions is needed. In the highest energy range of the CR spectrum, fluxes are too low for direct observation with satellites or balloon-borne instruments: ground based detectors are used. They observe the particle showers initiated by CRs when interacting with the terrestrial atmosphere. From the point of view of particle physics, the detection of CRs at extreme energies can be regarded as a fixed target collider experiment. The first interactions between primary CRs and atmospheric nuclei reach energies equivalent to p-p collisions at $\sqrt{s} \simeq 400$ TeV, about one order of magnitude above those accessible with the LHC.

2 The Pierre Auger Observatory

The Pierre Auger Observatory operates in the Ultra High Energy (UHE) range ($E > 10^{18}$ eV). Its Southern Site is located in the Mendoza province, in Argentina. The Auger Observatory is a hybrid experiment combining two complementary detection techniques. A 3,000 km² surface detector (SD) samples the shower particles reaching ground level with 1660 water-Cherenkov detectors. The SD is overlooked by a fluorescence detector¹ (FD): 27 telescopes at 4 sites detect the fluorescence light emitted along the longitudinal path of the shower. The SD has $\sim 100\%$ duty cycle, and detection efficiency $> 97\%$ above 3 EeV for zenith angles $< 60^\circ$.² The signal in each water-Cherenkov detector is recorded as FADC traces from 3 photomultipliers. The FD,

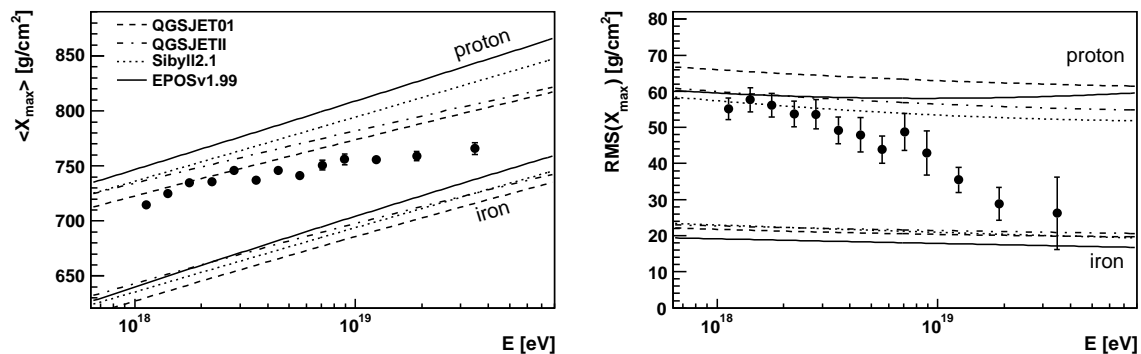


Figure 1: The measured X_{\max} and $\text{RMS}(X_{\max})$ as a function of the primary energy are compared with air shower simulations using different primary particles and hadronic interaction models. The $\text{RMS}(X_{\max})$ distribution is obtained after subtracting in quadrature the detector resolution.⁶

21 which operates in clear moonless nights (duty cycle $\sim 15\%$), can detect CRs down to an energy
 22 of $\sim 10^{18}$ eV and is able to observe, within its field of view, the longitudinal profile of the
 23 shower. The coexistence of the two detectors combines the high exposure of the SD, yielding
 24 high statistics, and the almost calorimetric measurement of the energy of air showers provided
 25 by the FD. A subset of high quality hybrid events (golden hybrids), detected and reconstructed
 26 independently by the SD and FD, are used to calibrate the SD energy scale on the FD one.³ The
 27 estimate of the total systematic uncertainty on the energy scale is 22% .⁴

28 3 Measurements of X_{\max}

29 The depth at which the longitudinal development of the shower reaches its maximum contains
 30 information about the mass of the primary CR initiating the shower and about the properties
 31 of hadronic interactions. It can be measured with high accuracy by the FD. The average value
 32 $\langle X_{\max} \rangle$ depends on the primary energy E and on the number of nucleons A :

$$\langle X_{\max} \rangle = \alpha (\ln E - \langle \ln A \rangle) + \beta, \quad (1)$$

33 with α and β depending on the details of hadronic interactions. Their values are very
 34 sensitive to changes in cross-section, multiplicity and elasticity.⁵ Eq. 1 is derived from a simple
 35 generalization of the Heitler model to showers induced by hadronic primaries, but it provides a
 36 good description of the X_{\max} evolution predicted by hadronic models currently in use. In the
 37 energy range of interest for the Auger Observatory, α and β can be considered independent of E .
 38 Another mass sensitive quantity is $\text{RMS}(X_{\max})$, expressing quantitatively the shower-to-shower
 39 fluctuations of X_{\max} . It is expected to decrease with the number of nucleons A . The measurement
 40 of X_{\max} and $\text{RMS}(X_{\max})$ presented in Fig. 1 is based on the analysis of hybrid data collected
 41 between December 2004 and March 2009⁶. Hybrids are defined as events observed by the FD and
 42 at least one SD station. After quality cuts, 3754 hybrid events are used. The number of events
 43 per energy bin is shown in Fig. 2, left. A comparison with four widely used high-energy hadronic
 44 interaction models^{7,8,9,10} suggests a gradual transition to heavier composition with increasing
 45 primary energy (Fig. 1, left). In the simple hypothesis of two mass components, however, the
 46 $\text{RMS}(X_{\max})$ results from the RMS of individual species and from the separation of their $\langle X_{\max} \rangle$:
 47 a gradual transition from p to Fe primaries should lead to an increase of $\text{RMS}(X_{\max})$ above the
 48 value predicted for protons.¹¹ This effect is not observed in the Auger measurements (Fig. 1,
 49 right).

50 The elongation rate, defined as the variation of X_{\max} per decade of energy, is sensitive to changes
 51 in composition with energy. A constant elongation rate cannot describe the measured evolution
 52 of $\langle X_{\max} \rangle$ with energy. A broken line is used in Fig. 2 (left) to fit the distribution: a change of

53 82_{-21}^{+25} g/cm²/decade in the elongation rate occurs at $\log_{10}(E/\text{eV})=18.24 \pm 0.05$. This is close
 54 to the energy of the spectral ankle³ at $\log_{10}(E_{\text{ankle}}/\text{eV})=18.65 \pm 0.09(\text{stat})_{-0.11}^{+0.10}(\text{sys})$, which is
 55 usually interpreted in terms of transition from galactic to extragalactic CRs. This interpretation
 56 is supported by the observed change in the elongation rate, under the assumption that hadronic
 57 interactions are not significantly changing with energy.

58 4 Muon content of air showers

59 The sensitivity of the Auger Observatory to both the electromagnetic and muonic components
 60 of air showers, allows us to test predictions of their relative contributions given by hadronic
 61 interaction models. The detector cannot, at present, measure separately the muon content of
 62 air showers, but several methods have been developed for an indirect estimate of the contribution:

- 63 (a) the **universality method**¹², based on the hypothesis that the electromagnetic and muonic
 64 signals measured at the ground for a fixed energy and a given distance from the shower axis
 65 have a universal dependence on the difference in grammage between the observation level
 66 and the shower maximum. The relative normalization of the muonic component can then
 67 be determined by requiring the total signal to match the experimental observations;
- 68 (b) the **jump method**¹³ correlates the signal differences between consecutive bins of the SD
 69 FADC traces and the muon fraction of the total signal;
- 70 (c) the **smoothing method**¹⁴ finds muon-induced peaks in the FADC traces of the SD stations
 71 through an iterative smoothing procedure;
- 72 (d) the **golden hybrid analysis**¹⁴ selects, in a set of simulations with the same energy and
 73 geometry of a given event, the longitudinal profile that matches most closely the measured
 74 one. The simulated SD response is then compared with the SD measurement.

75 Events selected in the energy range $\log_{10}(E/\text{eV}) = 19 \pm 0.2$ ($\sqrt{s} \simeq 140$ TeV for proton primaries)
 76 and zenith $\theta < 50^\circ$ have been analysed to obtain the muonic content at 1000 m from the shower
 77 axis.¹⁴ The number of muons N_μ^{rel} relative to the prediction of QGSjetII⁹ for protons is shown in
 78 Fig. 2 (right). The results obtained with the different methods are compatible with each other.

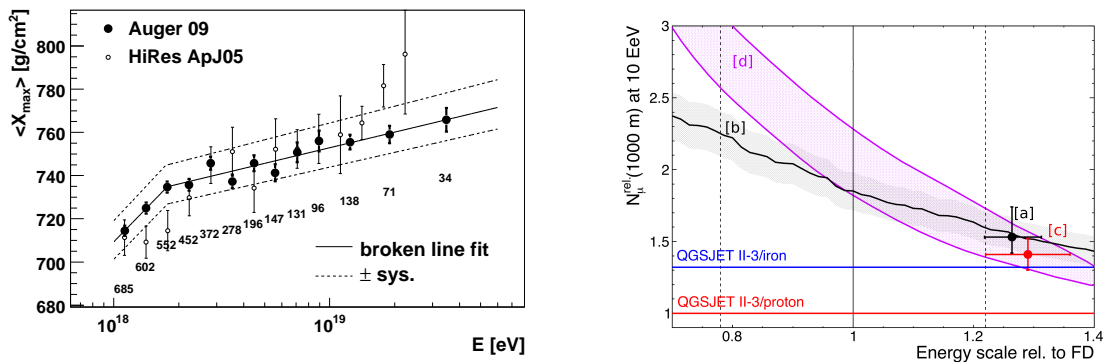


Figure 2: Left: A broken line is used to fit the evolution of $\langle X_{\text{max}} \rangle$ with the logarithm of the primary energy. The change of slope (elongation rate) supports a change in the mass composition of cosmic rays at the ankle. The measurements of X_{max} published by the HiRes collaboration¹⁵ are shown for comparison. Right: The muon content of $E=10^{19 \pm 0.2}$ eV air showers is determined at 1000 m from the shower axis with different indirect methods (a-d, see text and references therein) and expressed as a number relative to the prediction of the QGSjetII model for protons primaries. That number is shown as a function of the shift in energy scale with respect to the FD one.

79 Methods (a) and (c) constrain the energy scale to values higher than the FD scale but compatible
80 with its systematic uncertainty. If the energy is fixed at this new scale, the muon content in the
81 data exceeds the QGSjetII prediction for protons by 30% to 70%. The model prediction for iron
82 primaries ($N_{\mu}^{rel} = 1.32$, blue horizontal line) is marginally compatible with the results of the
83 methods within their systematic uncertainties. The measurement of X_{max} at the same energy,
84 however, is not compatible with QGSjetII predictions for a pure iron composition (Sec. 3).
85 The AMIGA¹⁶ extension of the Auger Observatory (in R&D) will employ scintillation counters
86 buried 2.3 m underground to avoid the detection of the electromagnetic component of air show-
87 ers. AMIGA will provide, on a fraction of the SD area, a direct measurement of the muonic
88 component that can be used to test and calibrate the indirect methods used so far.

89 5 Conclusions

90 The Pierre Auger Observatory is the largest detector currently in operation for the detection of
91 cosmic rays in the UHE range. Its main scientific goal, from the point of view of astrophysics, is
92 to find clues about the sources, acceleration and propagation of cosmic rays. From the point of
93 view of particle physics, it observes, through air showers, collisions up to $\sqrt{s} \simeq 400$ TeV, where
94 the properties of particle interactions have large uncertainties and are extrapolated from collider
95 measurements using hadronic interaction models. On the one hand reliable models are required
96 for a precise interpretation of data, in particular for determining the mass composition of CRs,
97 on the other hand the data collected with the Auger Observatory provide a unique test bed
98 for constraining model predictions at extreme energies. The depth of the shower maximum, its
99 fluctuations and the muon content of showers at ground level are important observables related
100 to the elemental composition and are model dependent. The measurement of X_{max} suggests a
101 transition toward increasingly heavier primaries with increasing energies, although the measured
102 $RMS(X_{max})$ is smaller than models would predict. The QGSjetII model was tested against data:
103 at $\sim 10^{19}$ eV it fails to describe consistently both X_{max} and muon content at 1000 m from the
104 axis. A deficit of muons is found in the predictions of the QGSjetII model.

105 References

- 106 1. The Pierre Auger Coll., *Nucl. Instrum. Methods A* **620**, 227 (2010).
- 107 2. The Pierre Auger Coll., *Nucl. Instrum. Methods A* **613**, 29 (2010).
- 108 3. The Pierre Auger Coll., *Phys. Lett. B* **685**, 239 (2010).
- 109 4. C. Di Giulio [Pierre Auger Coll.], Proc. of 31st ICRC (2009) arXiv:0906.2189.
- 110 5. R. Ulrich, *Phys. Rev. D* **83**, 054026 (2011).
- 111 6. The Pierre Auger Coll., *Phys. Rev. Lett.* **104**, 091101 (2010).
- 112 7. E. -J. Ahn *et al.*, *Phys. Rev. D* **80**, 094003 (2009).
- 113 8. N.N. Kalmykov and S.S. Ostapchenko, *Phys. Atom. Nucl.* **56**, 346 (1993).
- 114 9. S.S. Ostapchenko, *Nucl. Phys. Proc. Suppl.* **151**, 143 (2006).
- 115 10. T. Pierog and K. Werner, *Phys. Rev. Lett.* **101**, 171101 (2008).
- 116 11. M. Unger [Pierre Auger Coll.], Proc. of UHECR2010 (2010) arXiv:1103.5857.
- 117 12. F. Schmidt *et al.*, *Astropart. Phys.* **29**, 355 (2008).
- 118 13. M. Healy [Pierre Auger Coll.], Proc. of 30th ICRC (2007) vol. 4, p. 377.
- 119 14. A. Castellina [Pierre Auger Coll.], Proc. of 31st ICRC (2009), arXiv:0906.2319.
- 120 15. The HiRes Coll., *Phys. Rev. Lett.* **100**, 101101 (2008).
- 121 16. M. Platino [Pierre Auger Coll.], Proc. of 31st ICRC (2009) arXiv:0906.2354.